DEUTSCHES ELEKTRONEN-SYNCHROTRON DESY

DESY SR-71/10
December 1971

DESY-Bibliothek
21. JAN. 1972

The Optical Absorption of MgF_2, $MgCl_2$ and $MgBr_2$ in the Vicinity of the Mg L-Shell Transitions

by

P. Rabe, B. Sonntag, T. Sagawa, and R. Haensel
Deutsches Elektronen-Synchrotron DESY, Hamburg

and

II. Institut für Experimentalphysik der Universität Hamburg

2 HAMBURG 52 · NOTKESTIEG 1

To be sure that your preprints are promptly included in the HIGH ENERGY PHYSICS INDEX, send them to the following address (if possible by air mail):

DESY
Bibliothek
2 Hamburg 52
Notkestieg 1
Germany

The Optical Absorption of MgF_2, $MgCl_2$ and $MgBr_2$ in the Vicinity of the Mg L-shell transitions

P. Rabe, B. Sonntag, T. Sagawa[+], and R. Haensel

Deutsches Elektronen-Synchrotron DESY, Hamburg, Germany

and

II. Institut für Experimentalphysik der Universität Hamburg

Hamburg, Germany

The Mg^{++} $L_{II,III}$ absorption spectra of evaporated thin films of MgF_2, $MgCl_2$ and $MgBr_2$ have been measured in the energy range from 50 to 150 eV. Sharp absorption bands due to excitons were found at the onset of transitions from the 2p shell of Mg^{++} around 52 eV. At higher energies transitions from the 3d level of Br^- and from the 2s level of Mg^{++} show up as absorption maxima. The spectra are compared with those of metallic Mg, and the corresponding alkali halides. The measurements were performed by using the synchrotron radiation of the electron synchrotron DESY.

submitted to Physica Status Solidi

I. INTRODUCTION

Whereas the optical properties of the alkali halides have, to a great extent, been studied experimentally and theoretically, much less has been done with alkaline earth halides. Only semiempiric electron energy diagrams exist for the fluoride lattice[1,2,4]. The lack of theoretical band calculations can be explained by the fact that the alkaline earth halides have more than 2 atoms in the unit cell. As far as we know optical measurements on the Mg-halides have only been performed on MgF_2[3,4]. Besides the optical measurements electron energy loss measurements have also been done on MgF_2[5,6].

In the highly ionic earth alkali halides the valence band is formed by the outermost p electrons of the halogen ion. The outermost electrons of the alkaline earth ions are the 2p electrons for Mg^{++}, the 3p electrons for Ca^{++}, the 4p electrons for Sr^{++} and the 5p electrons for Ba^{++}. The binding energies of these electrons in the free atoms are: Mg 2p 51.4 eV, Ca 3p 25.4 eV, Sr 4p 19.9 eV, Ba 5p 14.6 eV[7].

Recently, optical measurements on CaF_2, SrF_2 and BaF_2 have been performed which cover the region of the metal core shell excitation up to 35 eV[8,9]. In order to look for the corresponding transitions in the Mg-halides we have made thin film absorption measurements of MgF_2, $MgCl_2$ and $MgBr_2$ in the energy range from 50 eV to 150 eV. Another impetus for these measurements came from measurements on metallic Mg in the same energy region[10].

In section II details of the experimental arrangement and the preparation of the samples are given. Section III gives the results of the measurements

and a discussion of the fine structure as well as a discussion of the continuum absorption related to the so-called delayed onset of $p \rightarrow d$ and $d \rightarrow f$ transitions.

II. EXPERIMENTAL METHOD AND SAMPLE PREPARATION

The thin film absorption measurements were performed using the 7.5 GeV electron synchrotron DESY as the light source[11,12]. The experimental set-up is shown in Fig. 1. The light coming from the synchrotron through a beam pipe of about 35 m length, is deflected by a grazing incidence plane mirror (PM), passes through the sample (S) and is then focused into the entrance slit (ES) of a grazing incidence spectrometer by a concave mirror. The gold coated grating of 1 m radius had 2400 lines/mm, a blaze angle of 4°16' and was used with an angle of incidence of 77°30' in the first order. The photomultiplier (PEM) was an open magnetic field type (Bendix M 306) and was mounted behind the exit slit, moving along the Rowland circle on a rotating arm (RA). The resolution was 0.1 Å over the entire spectrum. The signal from the photomuliplier was fed into the Y channel of a XY potentiometric recorder, with a reference signal proportional to the current in the accelerator. The beam current fluctuations were thus scaled down, so that all structures causing >3 % change in the absorption coefficient were easily observed. Both signals, before being fed into the XY recorder were amplified by lock-in amplifiers synchronized with the 25 cycles/second chopper wheel (CH). Thus the 50 cps noise was reduced.

The samples were mounted in front of the concave mirror. They were evaporated in situ from molybdenum baskets covered with Al_2O_3 onto carbon or aluminum foils[13], supported by a 75 µm copper mesh. The aluminum substrate also served as a prefilter in the energy range below 70 eV suppressing higher order light from the grating.

The evaporated Mg-halide foils transmitted about 10 % to 50 % of the incident light. Samples of different thicknesses were measured and the consistency of the results was checked. The errors due to stray light and higher spectral orders were thereby reduced.

During evaporation heavy mechanical stress formed in the evaporated films of MgF_2. The preparation of $MgCl_2$ and $MgBr_2$ films caused no problems. MgI_2 was obviously decomposed during evaporation and could, therefore, not be investigated.

The transmission of the empty substrate was measured before evaporation. The recorder plots of the spectra were digitalized and computer processed so as to obtain the absorption curves shown in Figs. 2 - 6. The relative consistency of the values in adjacent regions is about ±3 %.

Most of the measurements were performed at room temperature. Only the absorption structures at the onset of Mg^{++} 2p absorption were also measured at liquid nitrogen temperature.

III. EXPERIMENTAL RESULTS AND DISCUSSION

A. General Review of Absorption Curves

Figure 2 shows the absorption spectra of MgF_2, $MgCl_2$, and $MgBr_2$ in the energy range from 50 eV to 150 eV. Since the thickness of the Mg-halide films was not determined, the absorption coefficient is given in arbitrary units. The onset of Mg^{++} 2p-transitions can be seen by the appearance of fine structure near 50 eV. The fine structure is sitting on an absorption continuum, which must be due to transitions of outer electrons (valence band, F^-2s, Cl^-3s and Br^-4s) into higher energy states of the conduction band. The oscillator strength of this background absorption, as compared to the Mg^{++} 2p-absorption is much higher for MgF_2 than for $MgCl_2$ and $MgBr_2$.

The background absorption, which is due to the halogen ions, can be understood, at least qualitatively, by looking at the absorption of the corresponding iso-electronic rare gases Ne, Ar and Kr. The similarity of the absorption cross sections of atomic F and Ne, Cl and Ar and Br and Kr, as calculated by McGuire, support this procedure[14,15].

Measurements of the absorption of the solid and gaseous rare gases Ne, Ar, and Kr[16-32] show that the oscillator strength for transitions of the outer-most p and s electrons are not exhausted at 50 eV. The number of effective electrons contributing to absorption from the threshold up to 50 eV is 3 for Ne and 5 for Ar and Kr. These values are well below the number of 8 valence electrons per atom. The number of effective electrons contributing to the absorption of MgF_2 up to 48 eV has been determined by Stephan et al.[4] to be 9 electrons per molecule, that is 4.5 electrons per F^- ion.

The absolute cross section of Ne at 50 eV is 8 Mb decreasing monotonically to 2 Mb at 150 eV, whereas the absolute cross section of Ar in this energy range is around 1 Mb.

Above the onset of the Mg^{++} 2p transitions the absorption increases with energy, thus giving rise to a maximum at about 73 eV. This increase of absorption is less prominent in MgF_2 than in $MgCl_2$ because it is superimposed on the strong, decreasing background absorption discussed above. In $MgBr_2$ the maximum due to the Mg^{++} 2p-transitions is hidden by the onset of Br^- 3d transitions at 70 eV.

The increase of the absorption above the threshold, the maximum 20 eV above the onset and the following decrease of absorption to higher energies is in good agreement with the general shape of the absorption found for the 2p absorption of metallic Mg[10]. This is due to the delayed onset of 2p→d transitions as has been shown by McGuirès calculations for free Mg atoms[14,15]. For comparison the absorption spectrum of metallic Mg and the calculated cross sections are included in Fig. 5. The onset of Br^- 3d absorption at 70 eV in $MgBr_2$ gives rise to a further increase of absorption culminating at about 130 eV. This behaviour is very similar to that found for the 3d transitions of gaseous and solid Kr[16,17,32] (Kr 3d onset near 90 eV, absorption maximum at 190 eV) and the Rb-halides[33] (Rb 3d onset near 110 eV, absorption maximum in RbF and RbCl, where no superposition of the Br^- and I^- continuum absorption occurs, at ∿150 eV). This continuous absorption which follows the 3d fine structure near the threshold can be explained as a delayed onset of d→f transitions[34]. Above 89 eV where transitions from the 2s states of Mg^{++} may occur we find some prominent structures in $MgCl_2$ and $MgBr_2$, whereas in MgF_2 there is only a broad maximum.

The structures to be seen in the spectrum of MgF_2 are considerably broader than those in the spectra of $MgCl_2$ and $MgBr_2$. It is not clear whether this broadening is due to interactions of the final states with the strong underlying continuum or to the different crystalline structure (MgF_2 tetragonal, $MgCl_2$ and $MgBr_2$ hexagonal). It may also be related to a greater amount of crystalline disorder, since the preparation of the MgF_2 films showed that heavy mechanical stress exists in thin evaporated films of MgF_2. The fact that the structures of the absorption spectra of fluorides are broader than those of other halides has also been found for alkali fluorides, as for example RbF[33].

B. Fine Structure

Above the onset of the Mg^{++} 2p-transitions extending over the energy range up to about 100 eV we find a number of absorption maxima in the spectra of MgF_2, $MgCl_2$ and $MgBr_2$. The energy positions of these absorption peaks are given in Table I. At the onset of the 2p absorption of Mg^{++} in $MgCl_2$ and $MgBr_2$ there are two sharp maxima A^+_p and B^+_p. In MgF_2 only one maximum shows up. The profile and the energy position of the peaks A^+_p and B^+_p has also been measured at liquid nitrogen temperature. The resulting spectra are shown on an enlarged scale in Fig. 3. The energy separation between A^+_p and B^+_p is 0.38 eV in $MgBr_2$ and 0.41 eV in $MgCl_2$. The shape of the absorption peak B^+_p in MgF_2 is clearly asymmetric. We, therefore, think that it is also composed of two partners, but these partners could not be resolved, even at liquid nitrogen temperature. Going from $MgBr_2$ to $MgCl_2$ and to MgF_2 the half width of the peaks increases and the maxima shift to higher energies.
This general feature has also been found for alkali halides.

As there are no band calculations available one can only give a tentative interpretation. The valence band of the Mg-halides is due to the outermost p-electrons of the halogen ion. The lowest part of the conduction band is formed by the 3s states of Mg^{++}. We suppose that the minimum of the conduction band is at the point Γ at the center of the Brillouin zone and that the symmetry character of the wave functions at this point is of s-type. Transitions from the flat 2p states of Mg^{++} to the conduction band minimum are, therefore, optically allowed. Stephan et al.[4] interpreted the first maximum of ε_2 at 11.7 eV in MgF_2 as a transition of a 2p electron of F^- to an exciton state coupled to the conduction band. They found the onset of interband transitions at 12.2 eV.

Similarly, we think the maxima A_p^+ and B_p^+ being due to transitions of 2p electrons of Mg^{++} to excitonic states coupled to the s-symmetric minimum of the conduction band.

The corresponding transitions in the free Mg^{++} ion would be $2p^6 \rightarrow 2p^5 3s$. The electron configuration in the ground state is $^1S_0$. According to Shortley[35] the configuration $2p^5 3s$ is much closer to LS-coupling than to jl-coupling. Most of the oscillator strength is, therefore, concentrated on the transition $^1S_0 \rightarrow {}^1P_1$ at 53.50 eV. A weak intercombination line $^1S_0 \rightarrow {}^3P_1$ at 52.92 eV also exists. The resulting energy difference between these transitions is 0.58 eV. The experimental ratio of the oscillator strength of the maxima A_p^+ and B_p^+ leads to the suggestion that the maximum B_p^+ corresponds to the transition $^1S_0 \rightarrow {}^1P_1$, whereas the weaker maximum A_p^+ corresponds to the transition $^1S_0 \rightarrow {}^3P_1$.

The fact that the energy distance between A_p^+ and B_p^+ in $MgCl_2$ and $MgBr_2$ is smaller than 0.58 eV can be explained by a smaller exchange interaction between electron and hole in the Mg-halides, as compared to the free Mg^{++} ion.

Onodera and Toyozawa[36] showed that the exchange energy between electron and hole of an exciton and the value of the spin-orbit splitting of the associated state in the crystal can be calculated from the observed values of the intensity ratio and the separation between the components of the doublet. According to Onodera and Toyozawa[36] the following relations hold for Γ excitons:

$$\Delta E = \sqrt{(\Delta - \frac{\lambda}{3})^2 + \frac{8}{9}\lambda^2} \tag{1}$$

$$\operatorname{tg} 2\phi = \frac{2\sqrt{2}\Delta}{(3\lambda - \Delta)} \tag{2}$$

$$\frac{I_B}{I_A} = \frac{(\sqrt{\frac{1}{3}}\cos\phi + \sqrt{\frac{2}{3}}\sin\phi)^2}{(\sqrt{\frac{2}{3}}\cos\phi - \sqrt{\frac{1}{3}}\sin\phi)^2} \tag{3}$$

ΔE	energy difference between peak A and B
Δ	exchange energy
λ	spin orbit splitting
I_A, I_B	intensity of peak A, B

In order to get the intensity ratio I_B/I_A we had to separate the exciton band into two components by fitting the experimental curves measured at liquid nitrogen temperature (Fig. 3) by means of two theoretical distributions. Toyozawa[37] has pointed out that the shape of the exciton absorption band is Gaussian when the coupling between electrons and phonons is strong. The strong coupling occurs at high temperature, if many defects are present, or the effective mass of the exciton is large. In the case of weak coupling the exciton absorption band has an asymmetric Lorentzian shape. According to Toyozawa et al.[38] the coexistence of local and band aspects also cause the exciton line shape to

be asymmetric Lorentzian. Nakai et al.[39] have shown that the shape of the exciton found at the onset of the Na^+ 2p absorption in sodium halides is Gaussian at room temperature and Lorentzian at liquid nitrogen temperature. We, therefore, used asymmetric Lorentzian distributions to approximate the exciton bands A_p^+ and B_p^+ measured at liquid nitrogen temperature, but were unsuccessful. It turned out that the line shape of the maxima A_p^+ and B_p^+ is Gaussian. The experimental curves together with the calculated Gaussian distributions are shown in Fig. 3. The background absorption has been taken into account by a function of the type aE^k (E = photon energy). The large effective mass of the core excitons or the existence of many defects in the samples are possible explanations for this behaviour.

The values of the half widths of the maxima, the intensity ratios I_B/I_A, the energy differences ΔE, the exchange energies Δ and the spin-orbit splitting λ for MgF_2, $MgCl_2$ and $MgBr_2$ are given in Table II.

One should not take these experimental values too seriously because the substraction of the background absorption and the separation of the two peaks, especially in the case of MgF_2, could cause considerable errors.

The amounts of the spin orbit splitting of the Mg 2p level in $MgCl_2$ (0.30 eV) and $MgBr_2$ (0.27 eV) are in good agreement with the value calculated for atomic Mg[40] (0.32 eV). These values are also very close to the energy separation (0.27 eV) of the L_{II} and L_{III} edges in metallic Mg[41]. The intensity ratio of L_{II}:L_{III} is much closer to the 1:2 expected for pure jj coupling than the ratios I_B:I_A found for the Mg halides. All this leads to the supposition that the spin orbit splitting of the Mg 2p level is barely affected by the surroundings. The exchange energy is the same for MgF_2, $MgCl_2$ and $MgBr_2$. The fact that the exchange energy is not influenced by the halogen ions supports the assumption that

the excitons are fairly localized on the Mg^{++} ion.

One striking feature of the Mg^{++} $L_{II,III}$ absorption in Mg halides is the large oscillator strength of the exciton doublet. This has also been found for the Na^{+} $L_{II,III}$ absorption in sodium halides[39,42-44]. Nakai et al.[39] attributed this fact to the localization of the excitation. According to Toyozawa et al.[38] the strong localization of excitation makes the oscillator strength concentrate on exciton absorption.

Above the sharp excitonic maxima A_p^+ and B_p^+ there are a number of weak maxima (E_p^+ and G_p^+ for MgF_2, D_p^+ and E_p^+ for $MgCl_2$, C_p^+ and E_p^+ for $MgBr_2$). We think these maxima are due to interband transitions, probably to s-symmetric final states. The lowest d-symmetric final states in the conduction band give rise to the strong absorption maxima I_p^+ in MgF_2 and F_p^+ in $MgCl_2$ and $MgBr_2$. We find transitions to higher lying d-symmetric states in the conduction band around 70 eV in MgF_2 and around the maxima K_p^+ and M_p^+ in $MgCl_2$ and $MgBr_2$.

The general shape of the absorption spectra in this energy region is similar to the shape of the Na^{+} 2p absorption spectra of the sodium halides[39,42-44]. For comparison the absorption spectra of the sodium halides are included in Fig. 4-6. Whereas for the sodium halides band calculations[45-48] show that the first prominent peak D above the excitons A and B is due to the lowest d-symmetric states in the conduction band, the strong increase of absorption around F is due to higher lying d-symmetric final states. Going from MgF_2 to $MgCl_2$ and to $MgBr_2$ the d-symmetric conduction band states are shifted towards the conduction band minimum. This shift has also been found for the sodium halides where it is in good agreement with the results of the band calculations.

The onset of the 3d absorption of Br^- is at 70 eV in $MgBr_2$. The shape of the Br^- 3d absorption in MgBr is very similar to that found in RbBr[33]. The 3d absorption spectrum of Br^- in RbBr is included in Fig. 6. Figure 6 and Table I show that there is almost a one to one correspondence between the maxima A_d^- to I_d^- in $MgBr_2$ and those in RbBr. The spin-orbit splitting of the Br^- 3d level is about 1 eV. We, therefore, identify the pairs $(A_d^- B_d^-)$, $(C_d^- D_d^-)$ and $(E_d^- F_d^-)$ as spin-orbit mates.

The prominent maxima A_s^+ and B_s^+, which show up in the spectra of $MgCl_2$ and $MgBr_2$ are due to transitions from the 2s states of Mg^{++} to p-symmetric final states in the conduction band. The shape and the energy separation of these peaks are very similar to those of the F^- 2s transitions in MgF_2 given by Stephan et al.[4]. In MgF_2 there is only one broad maximum C_s^+ at 100.57 eV which could be caused by transitions of the Mg^{++} 2s electrons. Between 78 eV and 90 eV three maxima O, P and Q show up in the absorption spectrum of MgF_2, whereas we could find no structure in this energy region in $MgCl_2$. In $MgBr_2$ the Br^- 3d absorption dominates the absorption in this energy region. It is very improbable that the relative sharp maximum O, and also the maxima P and Q are due to transitions of Mg^{++} 2p electrons to conduction band states lying 25 eV above the bottom of the conduction band. On the other hand one could think of the following explanations.

According to Stephan et al.[4] the binding energy of the F^- 2s electrons in MgF_2 is about 29 eV. The energy necessary to excite one Mg^{++} 2p electron and one F^- 2s electron simultaneously is, therefore, about 84 eV. This is more than 4 eV higher than the experimental value of 79.36 eV for peak O. This energy shift may, for example, be explained by the Coulomb interaction between the two holes created by this process, whose energy is in the same order of magnitude. As

far as we know no calculation exists on the probability of such a process involving simultaneous excitation of two electrons well localized at different atoms. Taking into account the results of Hermanson[49] for the simultaneous production of two excitons by a single photon in alkali halides we would expect it to be orders of magnitude lower than for one-electron transitions. This contradicts the experimental results.

Another possible explanation is the simultaneous excitation of one Mg^{++} 2p electron plus one plasmon. The plasmon energy for MgF_2 is 24.6 eV[6]. The peaks O, P and Q could, therefore, be plasmon replicas of the peaks B_p^+, E_p^+ and I_p^+.

Even part of the maximum C_s^+ might be a plasmon replica of N_p^+. In principle such processes should be possible in soft X-ray absorption as well as in soft X-ray emission where plasmon satellites are well known. F.C. Brown et al.[50] have found a weak periodic structure in the Li^+ 1s absorption spectra in LiF, LiCl and LiBr which they explained as being an electron transition accompanied by the excitation of plasmons.

ACKNOWLEDGMENT

The authors are indebted to Dr. M. Skibowski for valuable discussions and to Mrs. E. Rabe for her help in operating the fitting program. Thanks are also due to the Deutsche Forschungsgemeinschaft for financial support.

References

+ Present address: Dept. of Physics, Tohoku University, Sendai, Japan

1. N.V. Starostin, Sov. Phys. Solid State 11, 1317 (1969)
2. see in
   T. Tomiki and T. Miyata, J.Phys.Soc. Japan 27, 658 (1969)
3. M.W. Williams, R.A. Mac Rae and E.T. Arakawa, J.Appl.Phys. 38, 1701 (1967)
4. G. Stephan, Y. Le Calvez, J.C. Lemonier and S. Robin, J.Phys.Chem. Solids 30, 601 (1969)
5. C. Gout, B. Lahaye and P. Perrier, Compt.Rend. B 265, 1460 (1967)
6. H. Venghaus, Opt.Comm. 2, 447 (1971)
7. J.A. Bearden and A.F. Burr, Rev.Mod.Phys. 39, 125 (1967)
8. G.W. Rubloff, J.Freeouf, H. Fritzsche and K. Murase, Phys.Rev. Letters 26, 1317 (1971)
9. W. Hayes, A.B. Kunz, and E.E. Koch, J.Phys. C 4, L200 (1971)
10. R. Haensel, G. Keitel, B. Sonntag, C. Kunz and P. Schreiber, phys.stat.sol. (a) 2, 85 (1970)
11. R. Haensel and C. Kunz, Z. Angew. Phys. 23, 276 (1967)
12. R.P. Godwin, in Springer Tracts in Modern Physics, edited by G. Höhler (Springer Verlag, Berlin, 1969), Vol. 51, p. 1
13. The foils were purchased from Yissum Research Development Co., Tel Aviv, Israel
14. E.J. McGuire, Phys.Rev. 175, 20 (1968)
15. E.J. McGuire, Research Report Sc-RR-70-721 November 1970 Sandia Laboratories
16. R. Haensel, G. Keitel, P. Schreiber and C. Kunz, Phys.Rev. 188, 1375 (1969)
17. P. Schreiber, Thesis University of Hamburg (1970), Internal report DESY F41-70/5

18. G. Keitel, Thesis University of Hamburg (1970) Internal report DESY F41-70/7

19. R. Haensel, G. Keitel, N. Kosuch, U. Nielsen und P. Schreiber, J. de Physique (to be published)

20. J.A.R. Samson, J.Opt.Soc.Am. 55, 935 (1965)

21. F.J. Comes and A. Elzer, Z. Naturforsch. 19a, 721 (1964)

22. D.L. Ederer and D.H. Tomboulian, Phys.Rev. 133, A 1525 (1963)

23. A.P. Lukirskii and T.M. Zimkina, Bull. Acad.Sci. USSR, Phys. Ser. 27, 808 (1963)

24. J.A.R. Samson, J.Opt.Soc.Am. 54, 420 (1964)

25. Po Lee and G.L. Weissler, Phys.Rev. 99, 540 (1955)

26. R.P. Madden, D.L. Ederer and K. Codling, Phys.Rev. 177, 136 (1969)

27. R.W. Alexander, D.L. Ederer, and D.H. Tomboulian, Bull.Am.Phys.Soc. 9, 626 (1964)

28. P. Metzger and G.R. Cook, J.Opt.Soc.Am. 55, 516 (1965)

29. R.E. Huffmann, Y. Tanaka and J.C. Larrabee, Appl.Opt. 2, 947 (1963)

30. J.A.R. Samson, Phys.Rev. 132, 2122 (1963)

31. O.P. Rustgi, E.I. Fischer and C.H. Fuller, J.Opt.Soc.Am. 54, 745 (1964)

32. A.P. Lukirskii, I.A. Brytov and T.M. Zimkina, Opt. Spectrosc. 17 234 (1964)

33. M. Cardona, R. Haensel, D.W. Lynch, and B. Sonntag, Phys.Rev. B 2, 1117 (1970)

34. U. Fano and J.W. Cooper, Rev.Mod. Phys. 40, 441 (1968)

35. see Mg III in C.E. Moore, Natl. Bur. Std. (U.S.) Circ. No. 467 (U.S. GPO, Washington, D.C.) Vol. I (1949) p. 109

36. Y. Onodera and Y. Toyozawa, J.Phys.Soc. of Japan 22, 833 (1967)

37. Y. Toyozawa, Progr. Theor. Phys. (Kyoto) 20, 53 (1958)

38. Y. Toyozawa, M. Inoue, T. Inui, M. Okazaki and E. Hanamura, J.Phys.Soc. Japan 22, 1337 (1967)

39. S. Nakai, T. Ishii and T. Sagawa, J.Phys.Soc. Japan 30, 428 (1971)

40. C.C. Lu, T.A. Carlson, F.B. Malik, T.C. Tucker, and C.W. Nestor, Jr., Atomic Data 3, 1-131 (1971)

41. C. Kunz, R. Haensel, G. Keitel, P. Schreiber and B. Sonntag, Proc. NBS Symposium on "Electronic Density of States", Nov. 1969 Washington, D.C. (to be published)

42. S. Nakai and T. Sagawa, J.Phys.Soc. Japan 26, 1427 (1969)

43. R. Haensel, C. Kunz, T. Sasaki and B. Sonntag, Phys.Rev. Letters 20, 1436 (1968)

44. F. Uzan, J.-Y. Roncin, V. Chandrasekharan and N. Damany-Astoin, Compt. Rend.B 267, 708 (1968)

45. A.B. Kunz, Phys.Rev. 175, 1147 (1968)

46. A.B. Kunz, phys.stat.sol. 29, 115 (1968)

47. N.O. Lipari and A.B. Kunz, Phys.Rev. B 3, 491 (1971)

48. A.B. Kunz, T. Miyakawa and W.B. Fowler, Mém.Soc.Roy.Sc.Lg., 5^{e} série, 20, 263 (1970)

49. J.C. Hermanson, Phys.Rev. 177, 1234 (1969)

50. F.C. Brown, C. Gähwiller, A.B. Kunz, and N.O. Lipari, Phys.Rev. Letters 25, 927 (1970)

Table Captions

Table I: Energy (in eV) of the peaks observed in the absorption spectra of MgF_2, $MgCl_2$ and $MgBr_2$ at room temperature. Energies measured at liquid nitrogen temperature are marked by LNT. Included are the binding energies for the free atoms[7] and the positions of the Br^- 3d absorption maxima[33].

Table II: Half width Γ, intensity ratio I_B/I_A, energy difference ΔE, exchange energy Δ, spin orbit splitting λ, of the excitons at the onset of the Mg^{++} $L_{II,III}$ absorption in MgF_2, $MgCl_2$ and $MgBr_2$. Values are obtained at liquid nitrogen temperature.

Table I

	Free atom			MgF_2	$MgCl_2$	$MgBr_2$	RbBr
Mg	L_{III}	52	A_p^+		53.57±0.02	53.08±0.02	LNT
			B_p^+	54.25±0.03	53.98±0.02	53.51±0.02	LNT
			C_p^+			54.58±0.05	
			D_p^+		55.32±0.05		
			E_p^+	55.92±0.1	56.30±0.1	55.73±0.07	
			F_p^+		57.55±0.05	57.13±0.05	
			G_p^+	58.53±0.4			
			H_p^+		60.62±0.3		
			I_p^+	61.75±0.15			
			K_p^+		63.58±0.1	63.5 ±0.15	
			L_p^+		64.74±0.1		
			M_p^+		66.24±0.1	65.5 ±0.2	
Br	M_V	69					
	M_{IV}	70					
			A_d^-			70.6 ±0.3	71.1
			B_d^-			72.41±0.05	72.1 ±0.2
			C_d^-			72.95±0.05	73.0 ±0.2
			N_p^+	73.65±0.3	72.81±0.9		
			D_d^-			73.80±0.05	73.9 ±0.2
			E_d^-			74.98±0.1	75.6 ±0.3
			F_d^-			76.70±0.2	76.7 ±0.7
			G_d^-				78.2 0.2
			O	79.36±0.1			
			P	80.99±0.2			
			H_d^-			82.50±0.3	82.9
			I_d^-			84.8 ±0.5	85.2±0.4
			Q	88.03±0.4			
			K_d^-			89.0 ±0.8	
Mg	L_I	89.5	A_s^+		95.18±0.15	94.53±0.1	
			B_s^+		97.84±0.2	96.96±0.2	
			C_e^+	100.57±1.0			
			R		107.70±1		
			S	129.10±2.0			

Material	Γ (eV)	I_B/I_A	ΔE (eV)	Δ (eV)	λ (eV)
MgF	A_p^+ 0.60	3.2	0.44	0.24	0.40
	B_p^+ 0.54				
MgCl	A_p^+ 0.30	6.1	0.41	0.28	0.30
	B_p^+ 0.32				
MgBr	A_p^+ 0.18	7.1	0.38	0.27	0.27
	B_p^+ 0.21				

Table II

Figure Captions

Fig. 1 Expermental set-up for thin film absorption measurements of MgF_2, $MgCl_2$ and $MgBr_2$. EO = electron orbit, V = valve, BS = beam shutter, PM = plane mirror, M = monitor signal electrode, CH = chopper wheel, S = sample, CM = concave mirror, ES = entrance slit, G = grating, PEM = photomultiplier, RA = rotating arm.

Fig. 2 Absorption spectra of MgF_2, $MgCl_2$ and $MgBr_2$ from 50 eV to 150 eV.

Fig. 3 Absorption spectra of MgF_2, $MgCl_2$ and $MgBr_2$ at the onset of $Mg^{++}2p$ transitions measured at liquid nitrogen temperature (solid line). Calculated Gaussian distributions (dashed line).

Fig. 4 Comparison between the Mg^{++} $L_{II,III}$ absorption spectrum of MgF_2 and Na^{+} $L_{II,III}$ absorption spectra of NaF. The energy scales have been appropriately shifted.

Fig. 5 Comparison between the Mg^{++} $L_{II,III}$ absorption spectrum of $MgCl_2$ and Na^{+} $L_{II,III}$ absorption spectra of NaCl. Included are the $L_{II,III}$ absorption spectrum of metallic Mg and the $L_{II,III}$ absorption spectrum of free Mg atoms as calculated by McGuire. The energy scales have been appropriately shifted.

Fig. 6 Comparison between the Mg^{++} $L_{II,III}$ absorption spectrum of $MgBr_2$ and Na^{+} $L_{II,III}$ absorption of NaBr. Included is the 3d Br^{-} absorption spectrum of RbBr. The energy scales have been appropriately shifted.

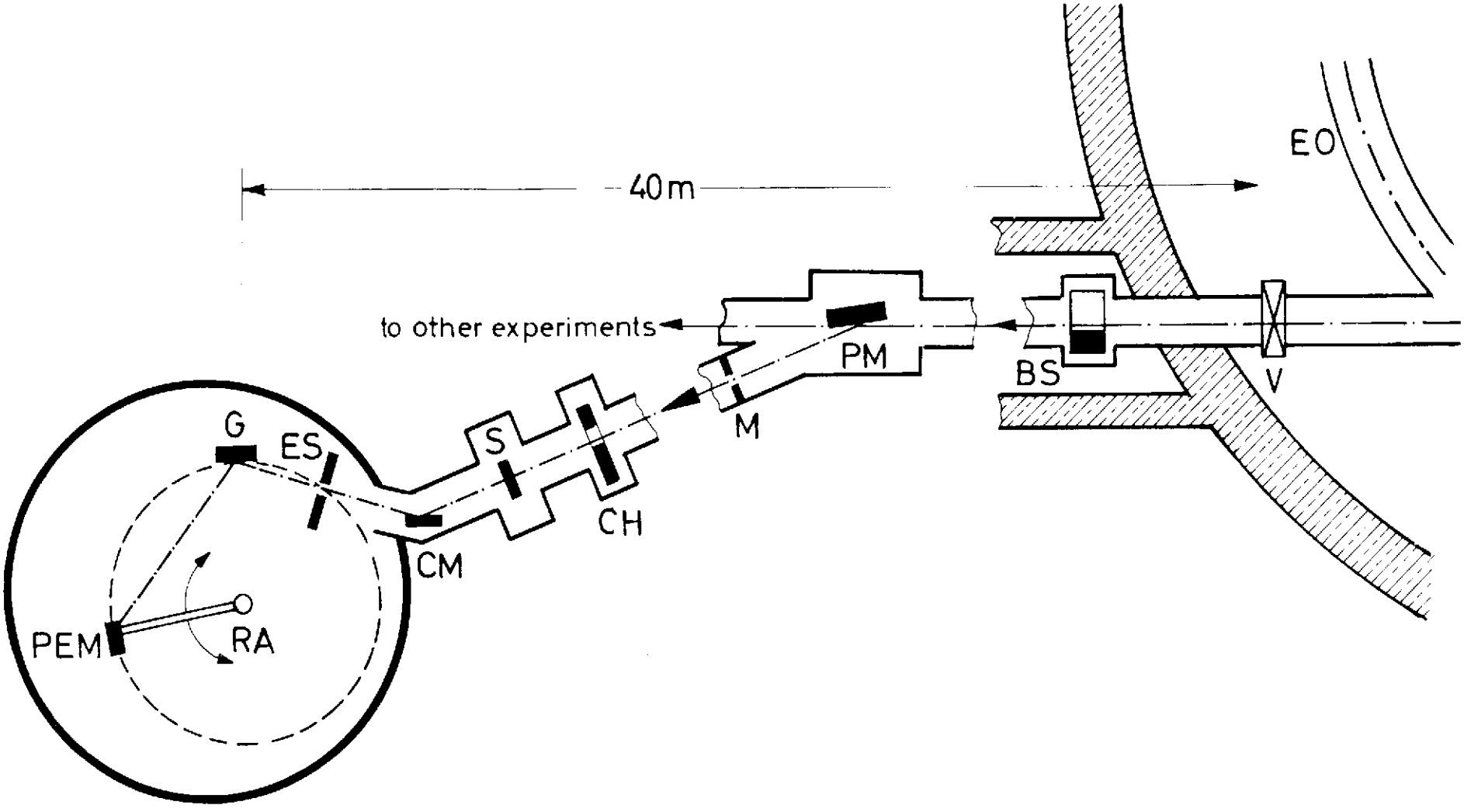

Fig.1

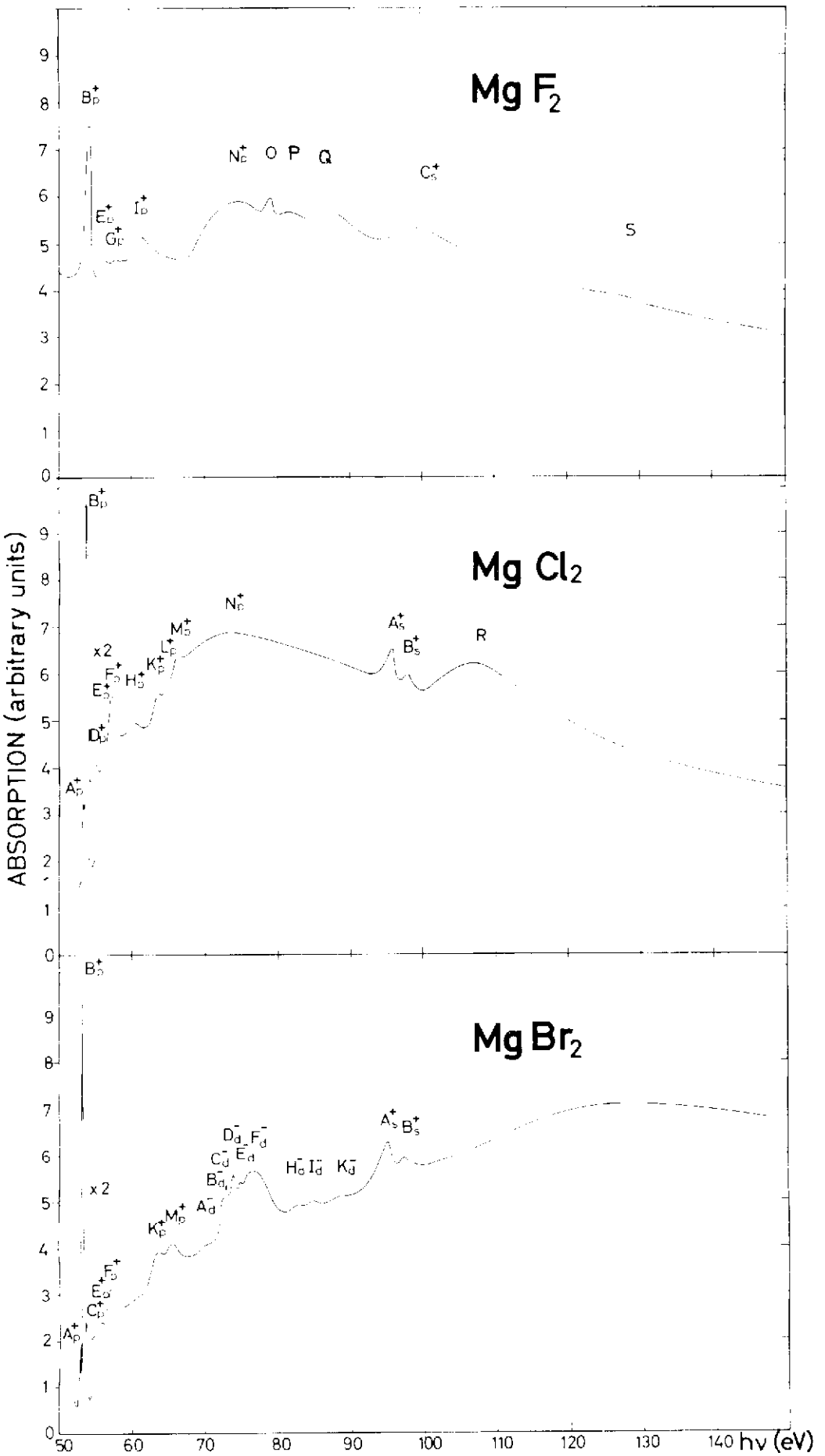

Fig.2

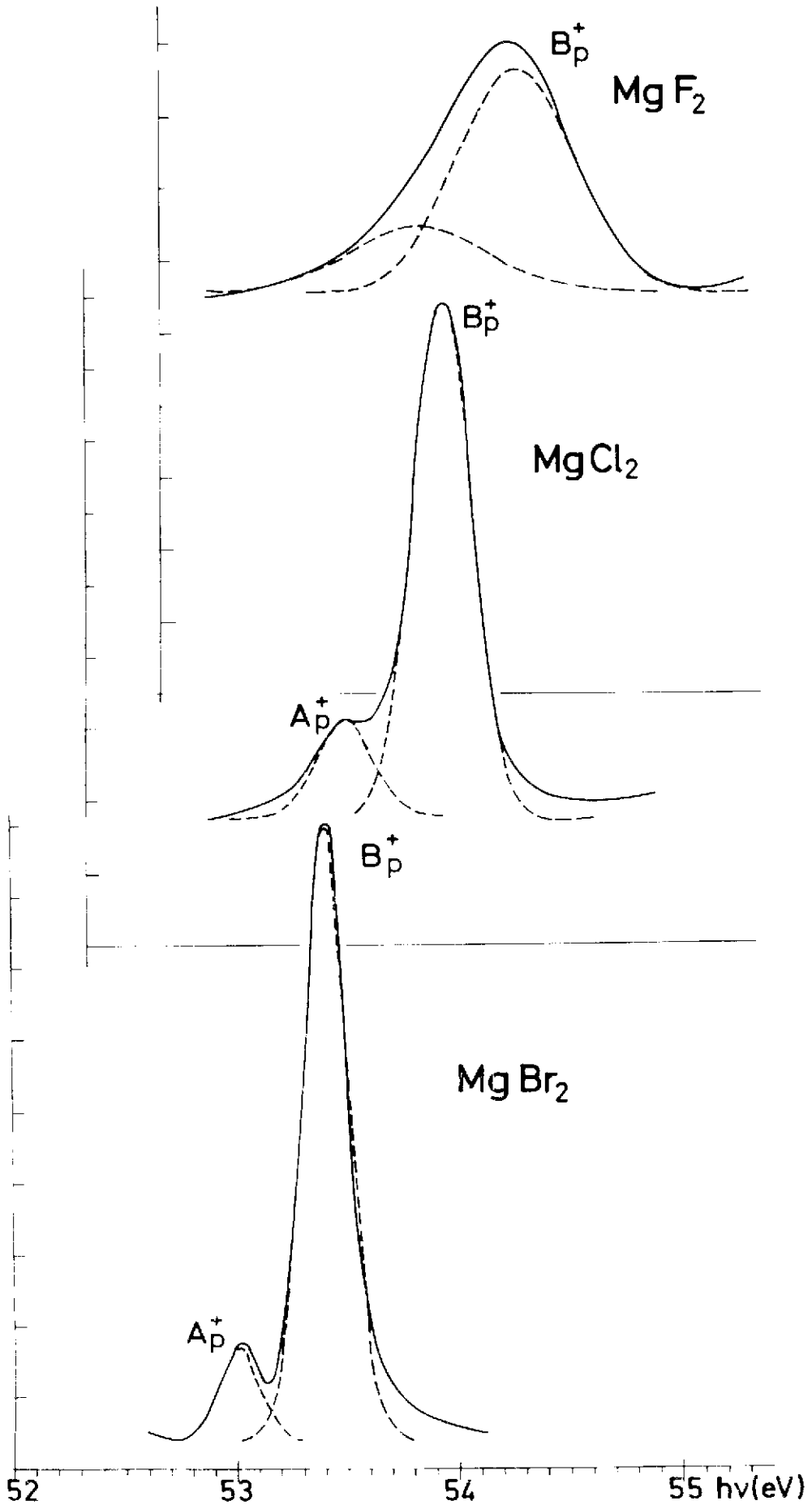

Fig.3

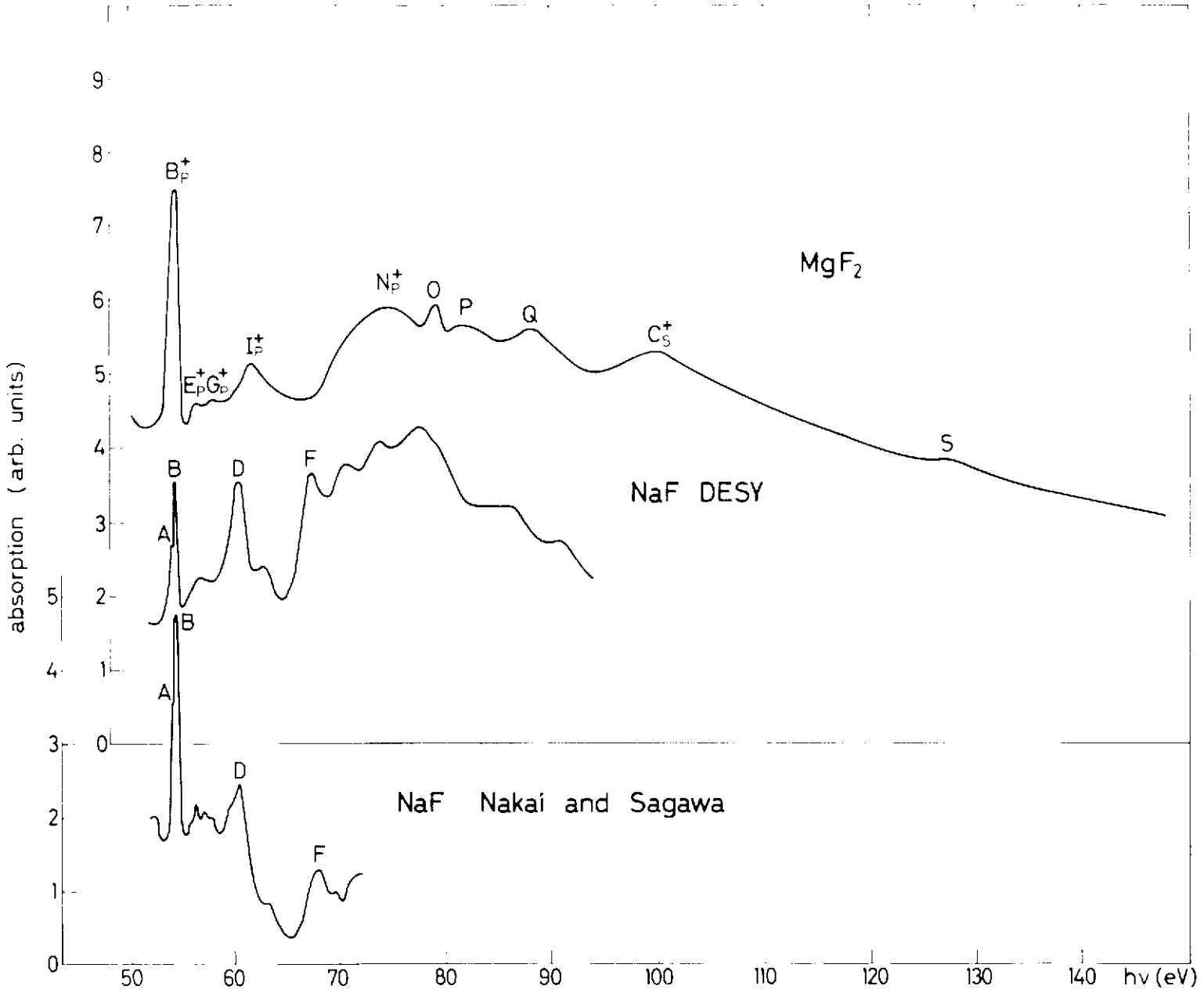
absorption (arb. units)
B_P^+
$E_P^+ G_P^+$
I_P^+
N_P^+
O
P
Q
C_S^+
S
MgF_2
B
D
F
A
NaF DESY
B
A
D
F
NaF Nakai and Sagawa
50
60
70
80
90
100
110
120
130
140
hν (eV)

Fig.4

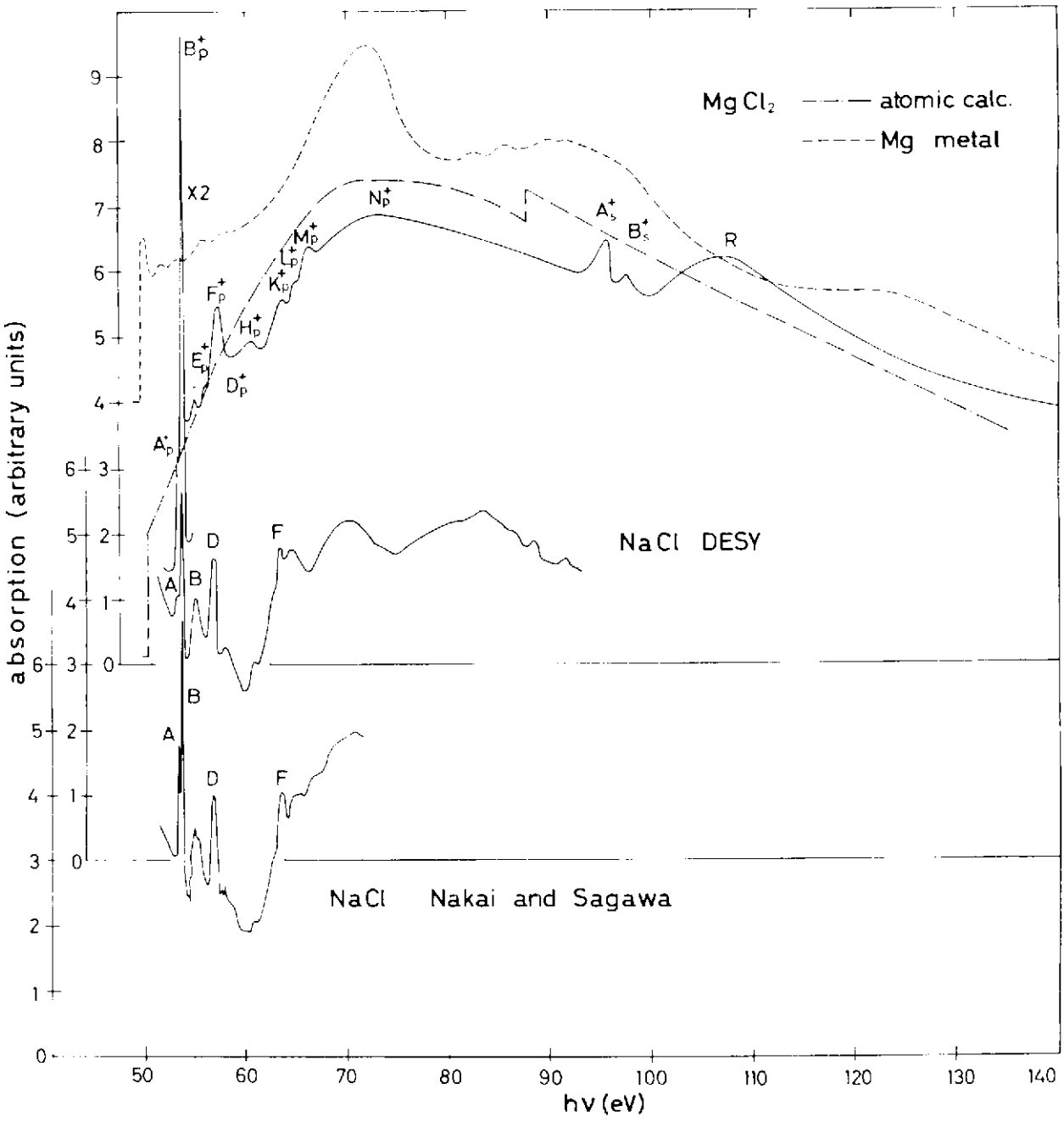
absorption (arbitrary units)
hν (eV)
Mg Cl₂
atomic calc.
Mg metal
NaCl DESY
NaCl Nakai and Sagawa
X2
B_p^+
N_p^+
A_s^+
B_s^+
R
M_p^+
L_p^+
K_p^+
F_p^+
H_p^+
E_p^+
D_p^+
A_p^+
A
B
D
F

Fig.5

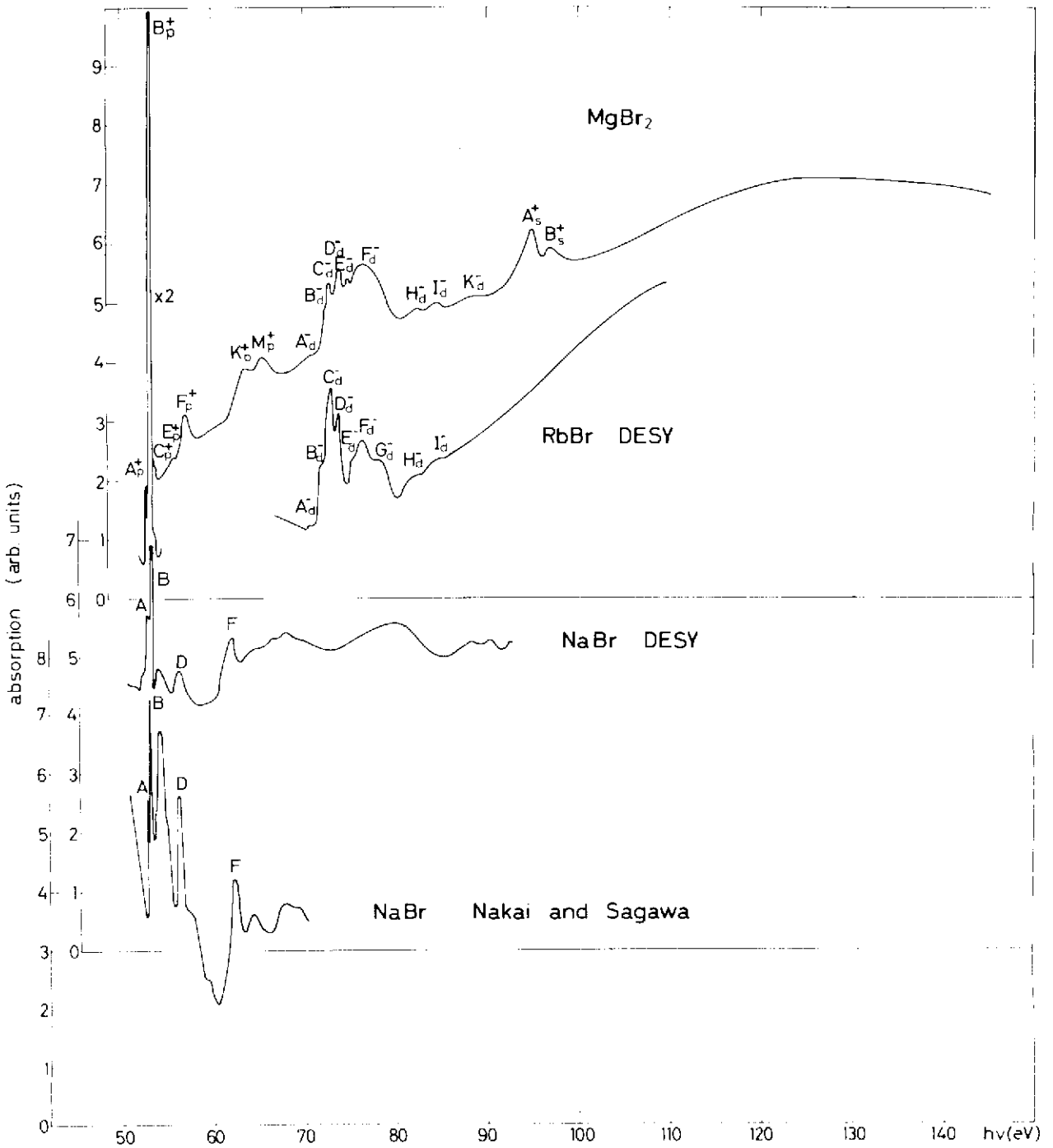
MgBr2
RbBr DESY
NaBr DESY
NaBr Nakai and Sagawa
absorption (arb. units)
hν(eV)
x2

Fig.6